

**PHOTOCATALYTIC DECOLOURISATION OF AZO DYES BY UNDOPED AND Cu
DOPED CdO NANOCRYSTALLINE THIN FILMS**

Dr.K.KaviARasu

¹Associate Professor, P.K.R Arts College for Women, Gobichettipalayam- 638 452, Tamilnadu.

² Research Scholar, Department of Physics, P.K.R Arts College for Women, Gobichettipalayam- 638 452,
Tamilnadu.

ABSTRACT:

Undoped and Cu doped Cadmium oxide (CdO) nanocrystalline thin films were synthesized by using chemical bath deposition method and annealed at 500°C. The films were characterized to study their structural, optical and compositional properties. The films were used to degrade the azo dyes, methylene blue (MB) and methyl orange (MO) using photo catalytic activity (PCA). It was found that the films were capable of degrading MB up to 15%.

Keywords: Cadmium oxide, Cu doped CdO, azo dyes, photo-catalytic activity

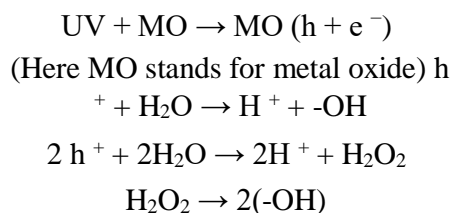
1. INTRODUCTION:

Organic chemicals, found as contaminants in wastewater effluents from manufacturing sources must be destroyed before discharging to the environment. Such pollutants may also be found in ground and surface waters which also need management to achieve suitable drinking water quality. Among various methods, photo catalysis has gained a lot of notice in the field of pollutant degradation.

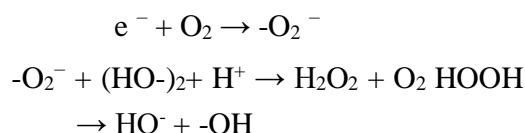
One of the major advantages of the photo catalytic process is that there is no additional requirement for secondary disposal methods. Another benefit is that when compared to other advanced oxidation technologies, especially those using oxidants such as hydrogen peroxide and ozone, expensive oxidizing chemicals are not required as ambient oxygen is the oxidant.⁽¹⁵⁾ Photo catalysts are also self-regenerated and can be reused or recycled.

Photo-catalysis is the acceleration of a photoreaction in the presence of a catalyst. In catalyzed photolysis, light is absorbed by an adsorbed substrate. In photo generated catalysis, the photo catalytic activity (PCA) depends on the capability of the catalyst to generate electron-hole pairs, which create free radicals (e.g. hydroxyl radicals: -OH) which are competent to experience secondary reactions. A reaction between the excited electrons with an oxidant to produce a reduced product to produce an

oxidized product takes place. Due to the generation of positive holes and electrons, oxidation-reduction reactions take place on the surface of semiconductors. In the oxidative reaction, the positive holes respond with the moisture present on the surface and create a hydroxyl radical. Oxidative reactions due to photo catalytic effect are as follows:



The reductive reaction due to photo catalytic effect:



Requirements for an efficient photo catalytic material include (i) an ability to generate electron-hole pairs, and prevent re-combination extended enough for the electrons and holes to arrive at the surface of the thin film, (ii) activation by sunlight (iii) inexpensive and easy to produce (iv) chemically inert (v) physically adherent and strong.

Henamsylvia Devi and Thiyam David Singh prepared Copper nanoparticles using *Centella asiatica* L. leaves extract at room temperature, for the photo catalytic degradation of methyl orange. These nanoparticles reduced methyl orange to its leuco form in aqueous medium in the absence of reducing agents. This catalytic effect of copper oxide nanoparticles contributed to its small size. Copper oxide nanoparticles such prepared had good catalytic properties.

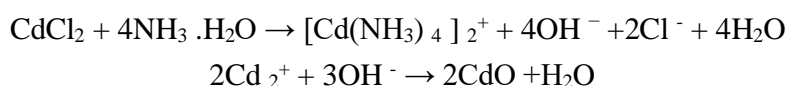
Beydoun et al⁽⁵⁾ gave an overview of the development and implications of nanotechnology in photo catalysis. The use of nanocrystalline thin films in electrochemically assisted photo catalytic processes.

2. EXPERIMENTAL METHODS

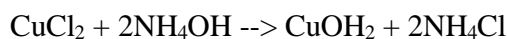
Synthesis of undoped and Cu doped CdO thin films

In the present work, Cadmium Oxide (CdO) thin films were prepared on glass substrates by sol-gel chemical bath deposition technique. In a conical flask, 0.1M of Cadmium chloride ($\text{CdCl}_2 \cdot \frac{1}{2}\text{H}_2\text{O}$) was dissolved in 250ml of deionized water. The solution was continuously

stirred by a magnetic stirrer for 1 hour to get a clear homogeneous solution. Ammonium hydroxide ($\text{NH}_3 \cdot \text{H}_2\text{O}$) solution was added with this solution drop wise till the pH is reached 12. The solution is taken in small beakers and the glass substrates were immersed into beakers for 24 hours. The glass slides were dried in hot air oven. These slides were annealed to 500°C . The undoped CdO thin film was prepared. The same procedure was continued to dope copper to CdO. Anhydrous Copper chloride (CuCl_2) was added to the undoped CdO precursor in the beaker⁽²⁾. As there was no appreciable change in the concentrations 1% to 3%, we took 4wt % and 8 wt% as optimal concentrations. This solution is stirred using a magnetic stirrer for 2 hours. The glass substrates were dipped into the beaker for 24 hours.



The glass substrates were dried finally, using hot air oven and annealed at 500°C . The copper doped nano crystalline thin films were thus synthesized.



Cu was chosen as dopant to organize and improve the properties of CdO thin films. The shrinkage of lattice constants after doping was due to the substitution of Cd by smaller Cu ions. The ionic radii of Cu and Cd are 0.73 \AA and 0.95 \AA , respectively, since copper has a smaller radius than that of Cadmium it may be easy for it to distribute in the host lattice [T. Aswani et al 2014]. Therefore, the decline in CdO lattice parameter with Cu doping can be explained by this difference in ionic radii. Generally speaking, the lattice parameters of a semiconductor depend on: (i) free electron concentration acting via deformation potential of a conduction-band minimum occupied by these electrons, (ii) concentration of foreign atoms and defects and their difference in ionic radii with respect to the substituted matrix ion, (iii) external strains for example, those induced by the substrate, (iv) temperature [Hakan Colak et al 2013]. The grain size and surface roughness of the CdO films could be controlled by higher Cu doping percentage. It was observed that the grain size of the films is decreased with increase in Cu doping [R.K. Gupta et al 2011]. The average grain size of 4% Cu doped CdO and 8% Cu doped CdO films is 75.43 and 39.25 respectively.

Photo-catalytic Activity Test

The photo catalytic activity of CdO nanoparticle can be studied using methylene blue

[C₁₆H₁₈ClN₃S] and methyl orange [C₁₄H₁₄N₃NaO₃S], the widely used azo dyes. The CdO thin films synthesized were dipped in methylene blue and methyl orange solutions. The methylene blue was examined by using a UV-Visible Spectrophotometer. The maximum absorption was found to be at a wavelength of 675nm. The maximum absorbance of MB is around 661nm- 665nm⁽⁶⁾ [Azzaryiatul Hafizah Amar, 2007]. Methyl orange solution was treated with the UV- Visible light, which gave a maximum absorption at a wavelength of 465nm. The maximum absorbance of methyl orange is approximately at 462nm in the visible region. The concentration of both dyes was prepared to be 10 ppm. Irradiation of the solutions was carried out under UV-Vis light (6 lamps with a power of 20 W, Philips).

The experiment was executed as follows: The maximum absorbance of both methylene blue solution and methyl orange solution were measured and then to that wavelength, absorbance was noted for the degradation of the dye before and after the addition of metal oxide. This absorbance is noted to be as A₀. After UV irradiation, the absorbance was again measured at 't' intervals of time. For every hour the absorbance value is noted. The total irradiation time is 5 hours. The extent of photo catalytic activity of CdO in methylene blue and methyl orange can be determined by measuring the absorbance of the solutions. The degradation of the dyes can be evaluated by using the formula:
Degradation (%) = $\frac{A_0 - A_t}{A_0} \times 100$

where A₀ represents the initial absorbance and A_t signifies the absorbance after t min reaction of the dyes at the characteristic absorption wavelength of 675 nm.

According to the principles of CdO photo catalyst, the energy gap are created on the surface of Cadmium oxide when are given radiation in photon light with either greater than or equaling the band gap energy, an electron may be advanced from the valence band to the conduction band (e⁻ c_b) leaving behind an electronic vacancy or "hole" in the valence band (h⁺ v_b). If charge separation is sustained, the electron and hole may transfer to the catalyst surface where they take part in redox reactions with the sorbed species.

3. RESULTS AND DISCUSSION

3.1. X-Ray Diffraction Analysis

The structural properties of CdO nano particles were investigated using an X-ray diffraction analysis. The existence of multiple diffraction peaks of (011), (111), (200), (220), (311) and (222) planes specifies the polycrystalline nature of the CdO with cubic structure ⁽⁷⁾ [Ngamnit Wongcharoen et al, 2012]. The XRD pattern exposed diffraction peaks approximately at 33°, 38°, 55.5° and 68° of 2θ values, indicating the hkl values as (1 1 1), (2 0 0), (2 2 0), and (2 2 2) which corresponds to polycrystalline having the characteristic peaks of face centered cubic structure of CdO (JCPDS Card No. 05-0640, 73-2245 and 78-065)^{(8),(9),(10),(11)} [Gbadebo Taofeek Yusuf et al 2016, Kumaravel et al 2010, Ngamnit Wongcharoen et al 2012, Saha et al 2007] and it is shown in Figure 1(a).

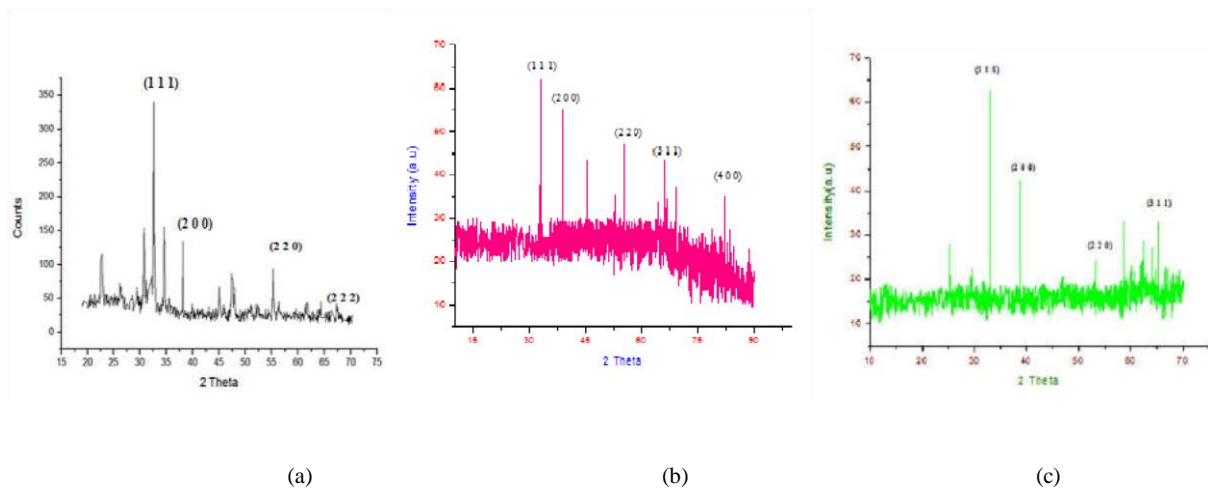


Fig. 1 XRD spectrum of (a) undoped CdO films (b) 4% Cu doped CdO thin films (c) 8% Cu doped CdO thin films

The sharp peak values are used to calculate the lattice parameter and grain size. The diffraction peaks of 4% Cu doped CdO observed at $2\theta = 32.8^\circ, 45^\circ, 47^\circ, 63^\circ, 81.5^\circ$. These peaks are associated with (1 1 1), (2 0 0), (2 2 0), (3 1 1) and (4 0 0) planes respectively. The grain size was estimated by the well-known Scherer's formula. The comparison of the observed XRD patterns with the standard JCPDS data (78-0653) confirms the face-centered cubic crystal structure.

Table:1 Structural values of CdO films

Film	2θ (deg)	FWHM (radians)	Lattice strain	Dislocation density ×10¹⁴ (δ) lines/m²	Micro strain(ε) (10⁴ lin⁻²m⁻⁴)	Average crystallite size (D) in nm
Undoped CdO	15.2526	0.3444	0.0225	17.1319	9.0365	38.76
	18.3321	0.1476	0.0080	03.1414	8.7565	
	22.6727	0.1968	0.0087	05.5651	6.8558	
	26.3868	0.5904	0.0223	49.9450	4.2314	
	29.0478	0.1476	0.0051	03.1105	5.5734	
Cu:CdO 4 wt%	31.8016	0.0974	0.0030	1.35019	5.28128	75.43
	62.6577	0.0900	0.0014	1.08983	2.81513	
	66.3824	0.1948	0.0029	5.05668	2.51643	
Cu:CdO 8%	18.2175	0.7793	0.0427	87.50736	4.87103	39.25
	20.2549	0.0974	0.0048	1.365705	8.21616	
	30.5658	0.3897	0.0127	21.65345	4.41862	

MORPHOLOGICAL ANALYSIS

SEM images of undoped and doped CdO thin films are shown in Figure 2. It can be seen that grains cluster together and hence do not display homogeneous distribution for both doped and undoped CdO samples, similar observations also reported by H. Colak et al 2013. The particles demonstrate uneven stone like shaped structure for Cu doped CdO nanopowder [T. Aswani et al 2014]. The grains seen in the SEM are the fields formed by the collection of nanosize crystallites [T. Aswani et al 2014]. It was observed that the grain size of the films is decreased with increase in Cu doping. The average grain size of pure CdO is 38.76, and for 4% Cu doped CdO, 8% Cu doped CdO films, it is found to be 75.43 and 39.25 nm, respectively. It is also evident from these microphotographs that the surface roughness of the films also decreases with increase in the Cu doping level. Thus, the grain size and surface coarseness of the CdO films could be restricted by Cu doping [R.K. Gupta et al 2011].

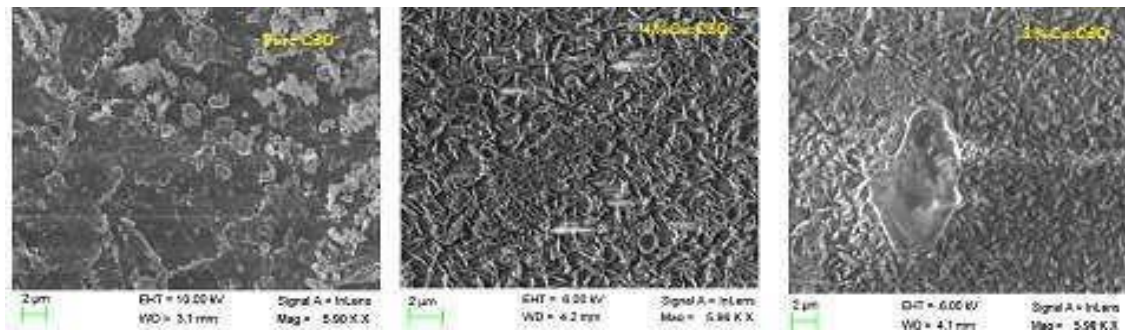


Fig. 2 SEM images of undoped CdO and Cu doped CdO thin films

PHOTO CATALYTIC DEGRADATION OF AZO DYES OF UNDOPED AND Cu DOPED CdO THIN FILMS

Fig.3 (a) shows the absorbance spectrum of methylene blue (MB) dye degradation using undoped Cadmium Oxide thin films under the irradiation of UV light. From the figure, it is clear that the absorbance of MB is more or less equal to 670nm. When the CdO thin films are dipped in the freshly prepared MB solution and kept under irradiation of UV light, it is monitored that the absorbance is considerably decreased. The irradiation time is varied from 1 hour to 5 hours. The absorbance value starts decreasing from the first hour of irradiation and at the fifth hour the absorbance is found to be reduced significantly. At the first hour of light irradiation, decolorizing efficiency for MB dye solution was achieved to about 11%. This value nearly reached 18% after 5h illumination. This result proves that the synthesized photo catalyst performs remarkably in removing the mentioned azo dyes under visible light illumination in a short time.

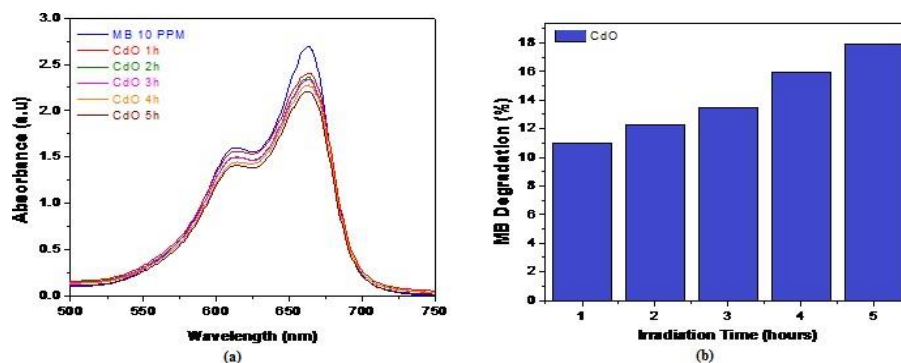


Fig.3. (a) Absorbance spectrum of MB dye degradation of undoped CdO thin films (b) Bar chart of MB degradation by undoped CdO.

In heterogeneous photo catalysis of azoic dyes, the electron-hole pairs will be primarily created by the irradiation of a semiconductor with a photon of energy equal to or better than its band gap width.⁽⁶⁾ The electrons and holes may drift to the semiconductors on the catalyst surface where they participate in redox reactions with the adsorbed azoic dyes.⁽²⁸⁾ The oxidizing radical could hit the azo dye molecule and disintegrate it into CO₂ and H₂O molecules which are non- hazardous.⁽²⁶⁾ It has been recommended that the formation of free radicals acts as a major oxidizing type.⁽⁷⁾ In the absence of catalyst, decolourization of MB and MO was not observed even after 24 hours, signifying that there was no direct oxidation path. On the other hand, decolourization of MB and MO happened only when CdO was brought into the solution mixtures indicating the essentiality of the films for promoting the decolourization which perhaps take place through free radicals pathway.

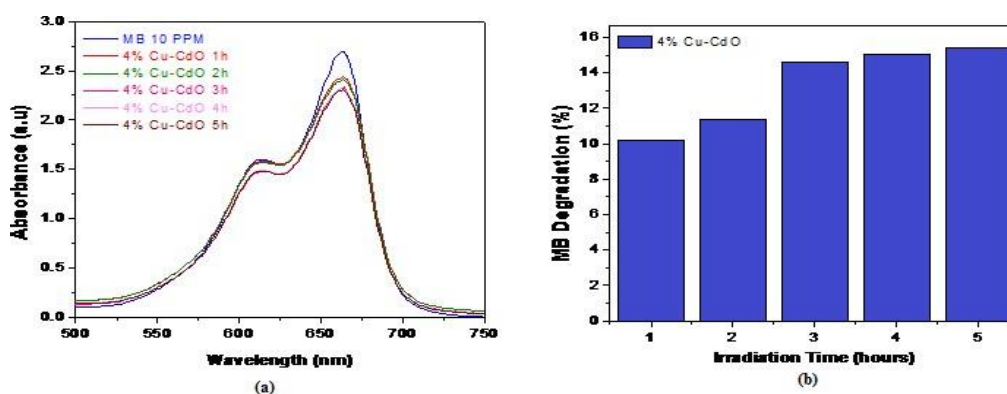


Fig. 4(a) Absorbance of Methylene blue by 4 wt%Cu doped CdO, (b) Bar chart of MB degradation by 4 wt% Cu doped CdO

The figures 4(a) and (b) demonstrate the absorbance of MB by the 4wt% Cu doped CdO thin films. To demonstrate the degradation process, the range was recorded at various time intervals.⁽²⁾ It can be obviously noticed, that the absorbance value of copper doped CdO nano thin films is reduced with time. With 4 wt% Cu doping films, the reduction of absorbance seems to be abrupt. At the first hour of irradiation time, there is an absorption of MB by 10%, but with time, only a minimum absorbance of MB takes place. After 5 hours of irradiation time, the absorption becomes 15%, beyond which there is no remarkable change.

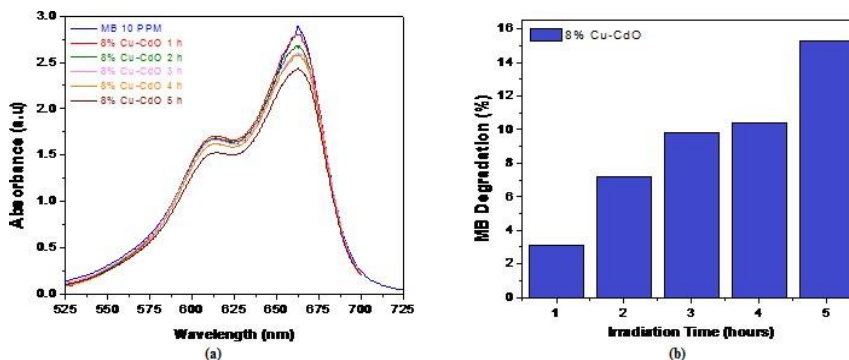


Fig. 5(a) Absorbance of Methylene blue by 8 wt%Cu doped CdO, (b) Bar chart of MB degradation by 8 wt% Cu doped CdO

The doping of 8wt% Cu to the cadmium oxide films improves the photocatalytic efficiency of the films, compared to the 4 wt% Cu doping. The figure 5 depicts the absorption efficiency of 8wt% Cu doped CdO films, with which, there is a gradual reduction in the absorbance value. Primarily with an irradiation of UV light for 1 hour, the degradation percentage is only 3%, but with an extension of time to about 5 hours, the percentage of deprivation is nearly 15%, which is 5 times the value when compared with the first hour of degradation.

Figure 6 (a) explains the absorbance spectrum of Methyl Orange (MO) by undoped CdO thin films. The absorbance of MO is at a wavelength of nearly 465nm in the visible light. When MO is treated with undoped CdO thin films, there is only a slight variation in the absorbance value. The introduction of the thin films may assist the formation of OH⁻ radical through which the degradation of the dye proceeds. In order to exhibit the degradation process, the spectra was recorded at different time intervals. ⁽²⁾

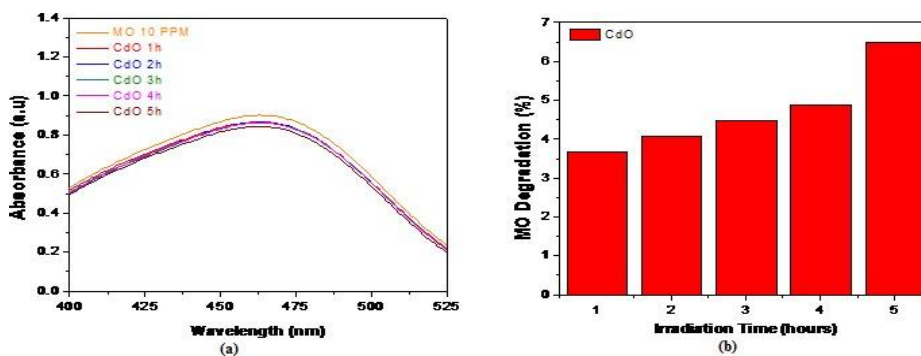


Fig.6. (a) Absorbance of Methyl orange by undoped CdO thin films (b) corresponding bar chart

In the absence of a photo catalyst, no degradation of azo dyes was observed under visible light irradiation.⁽⁴⁾ The obtained result is also shows that when the CdO thin films were not introduced, there was no degradation of MB and MO under UV and visible irradiation.

The absorbance of MO by Cu doped CdO thin films is explained by the figures 7 (a, b). When the copper doped nano thin films were used to find the absorbance of MO, the variation in it is found to be too small with 4 wt% Cu doped slides.

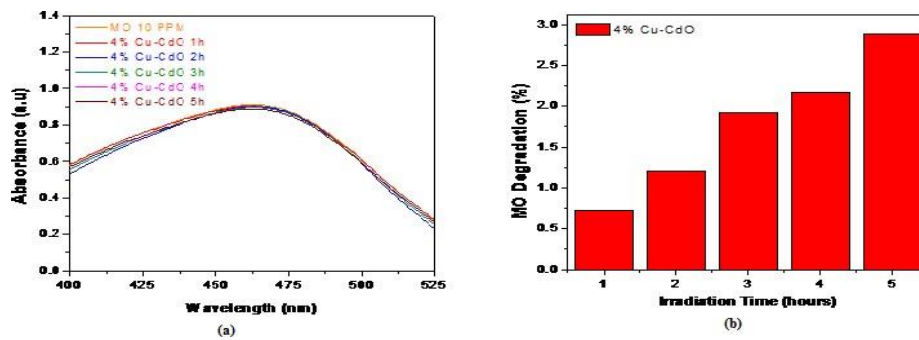


Fig. 7 (a) Absorbance of Methyl orange by 4 wt% Cu doped CdO films (b) corresponding bar diagram

Even though the irradiation time is extended to 5 hours, only a mild change is noted. But when 8 wt% Cu doped CdO films were used, the ability to absorb MO by the films seems to be dissimilar. After 1 hour of exposure to UV radiation, the value of absorbance appears to be diminished. 5 hours later, it is observed to get further reduced. At the end of 5 hours of radiation of light, the percentage of degradation is nearly 32.5%.

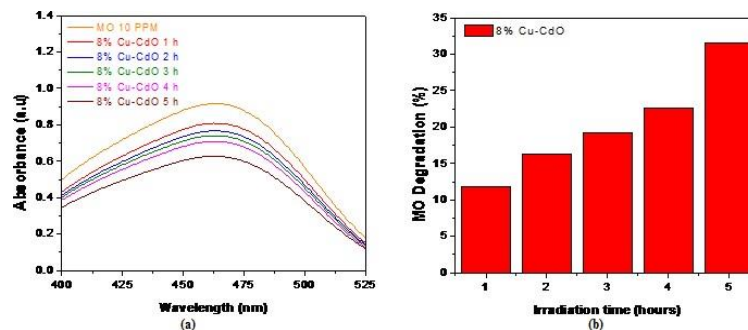


Fig. 8 (a) Absorbance of Methyl orange by 8 wt% Cu doped CdO films (b) corresponding bar diagram

This may be because of the enhanced coverage of the semiconductor surface by the metal which diminishes the adsorption sites on the surface, anticipated to be obtainable to the dye. Researchers have demonstrated that an enhanced photo catalytic activity of doped metal oxide is probably due to the acting of metal oxides to trap photo induced electrons, retarding the electron–hole recombination process, and thereby, promoting the photo degradation activity. Similarly, in this work, an enhanced photo catalytic activity of 4 wt% Cu doped CdO system may be due to the Cu atoms acting to trap photo induced electrons, delaying the process of electron–hole recombination, and so, might have promoted the photo degradation activity. The degradation percentage is calculated for MB and MO individually and is tabulated in Table 2 and Table 3. Table: 2 Degradation % of MB

MB Degradation- CdO					
	A₀	A_t	A₀-A_t	A₀-A_t/ A₀	(A₀-A_t/A₀)*100
1h	2.7015	2.4039	0.2976	0.110161	11.0161
2h	2.7015	2.3708	0.3307	0.122413	12.2413
3h	2.7015	2.3377	0.3638	0.134666	13.4665
4h	2.7015	2.2716	0.4299	0.159134	15.9134
5h	2.7015	2.2165	0.485	0.17953	17.9530
MB Degradation 4% Cu-CdO					
	A₀	A_t	A₀-A_t	A₀-A_t/ A₀	(A₀-A_t/A₀)*100
1h	2.7117	2.4361	0.2756	0.101634	10.16336615
2h	2.7117	2.403	0.3087	0.11384	11.38400266
3h	2.7117	2.3148	0.3969	0.146366	14.63657484
4h	2.7117	2.3038	0.4079	0.150422	15.04222443
5h	2.7117	2.2928	0.4189	0.154479	15.44787403
MB Degradation 8% Cu-CdO					
	A₀	A_t	A₀-A_t	A₀-A_t/ A₀	(A₀-A_t/A₀)*100

1h	2.8897	2.7905	0.0992	0.034329	3.432882306
2h	2.8897	2.6803	0.2094	0.072464	7.246426965
3h	2.8897	2.5811	0.3086	0.106793	10.67930927
4h	2.8897	2.559	0.3307	0.114441	11.44409454
5h	2.8897	2.4378	0.4519	0.156383	15.63830155

Table 3 Degradation % of MO

MO Degradation CdO					
	A₀	A_t	A₀-A_t	A₀-A_t/ A₀	(A₀-A_t/A₀)*100
1h	0.9039	0.8708	0.0331	0.036619	3.6619
2h	0.9039	0.8671	0.0368	0.040712	4.0712
3h	0.9039	0.8634	0.0405	0.044806	4.4805
4h	0.9039	0.8598	0.0441	0.048789	4.8788
5h	0.9039	0.8451	0.0588	0.065051	6.5051
MO Degradation 4% Cu-CdO					
	A₀	A_t	A₀-A_t	A₀-A_t/ A₀	(A₀-A_t/A₀)*100
1h	0.9131	0.9065	0.0066	0.007228	0.722812397
2h	0.9131	0.9021	0.011	0.012047	1.204687329
3h	0.9131	0.8955	0.0176	0.019275	1.927499726
4h	0.9131	0.8933	0.0198	0.021684	2.168437192
5h	0.9131	0.8867	0.0264	0.028912	2.891249589
MO Degradation 8% Cu-CdO					
	A₀	A_t	A₀-A_t	A₀-A_t/ A₀	(A₀-A_t/A₀)*100
1h	0.9128	0.8151	0.0977	0.107033	10.70333041
2h	0.9128	0.7688	0.144	0.157756	15.77563541
3h	0.9128	0.7431	0.1697	0.185911	18.59114812
4h	0.9128	0.7122	0.2006	0.219763	21.97633655
5h	0.9128	0.6351	0.2777	0.304229	30.42287467

Once the aqueous semiconductor (CdO) solutions are irradiated in light energy greater than the band gap energy of the semiconductors, conduction band electrons and valence band holes are produced.⁽¹⁴⁾⁽¹²⁾ As the charge separation is sustained, the electrons and holes may drift to the semiconductor surface where it takes part in the redox reaction with azo dyes.^{(10),(29),(9)} The electrons generated by light, react with the adsorbed dye molecules (O_2^-) on the semiconductor site and lessen it to superoxide radical anion (O_2^-) while the photo generated holes oxidize the H_2O or OH^- ions adsorbed at the semiconductor surface to OH^- radicals.^{(13),(23),(18)} These radicals generated with other highly oxidant species work as strong oxidizing agents which could easily hit the adsorbed azo dye molecules or those located close to the surface of the semiconductor, thus resulting in the degradation of azoic dyes.⁽¹⁶⁾ Thus in the present work also, the degradation of azoic dyes might have been caused by the redox reaction on the semiconductor surface.

4. CONCLUSION

The obtained results demonstrated that the undoped and doped CdO thin films can degrade azoic dyes (methylene blue and methyl orange) with optimum conditions. Methyl Orange dye is bleached to 32.5% by 8 wt% Cu doped cadmium oxide nano thin films when it is exposed to UV light.

Among the two different azoic dyes, methyl orange reacts better, degrading to the maximum of 32.5% in higher doping percentage of copper to the cadmium oxide nano thin films.

REFERENCES:

1. Ameen S, Akhtar MS, Nazim M, Shin HS, Mater. Lett. 96: 228-232, 2013.
2. Anouar Hajjaji, Atef Atyaoui, Khaled Trabelsi, Mosbah Amlouk, Latifa Bousselmi, Brahim Bessais, My Ali El Khakani, Mounir Gaidi, American Journal of Analytical Chemistry, 2014, 5, 473-482.
3. Ashok V. Borhade , Dipak R. Tope And Bhagwat K. Uphade, E-Journal of Chemistry, 2012, 9(2), 705-715.
4. Azadeh Tadjarodi, Mina Imani, Hamed Kerdari, Keyvan Bijanzad, Dorsan Khaledi and Maryam Rad, Nanomaterials and Nanotechnology, 2014.
5. Beydoun D., R. Amal, G. Low & S. McEvoy, World Congress on Particle Technology 3, 6–9 July 1998, Brighton, UK, Paper no. 385.
6. M. Cheng, M. Zhu, Y. Du, and P. Yang, International Journal of Hydrogen Energy, vol.

- 38, pp. 8631–8638, 2013.
7. R. Comparelli, E. Fanizza, M. L. Curri, P. D. Cozzoli, G. Mascolo, and A. Agostiano, *Applied Catalysis B*, vol. 60, no. 1-2, pp. 1–11, 2005.
 8. A. Fatemeh, F. Nazanin, and M. A. Tehrani Ramin, *Research Journal of Chemistry and Environment*, vol. 17, pp. 92–96, 2013.
 9. M. Hamadani, M. Behpour, A. S. Razavian, and V. Habbari, *Journal of Experimental Nanoscience*, vol. 8, pp. 901–912, 2013.
 10. F. A. Harraz, R. M. Mohamed, M. M. Rashad, Y. C. Wang, and W. Sigmund, *Ceramics International*, vol. 40, pp. 375–384, 2014.
 11. F. H. Hussein, *Asian Journal of Chemistry*, vol. 25, pp. 9393–9400, 2013.
 12. T. Jiang, L. Zhang, M. Ji et al., *Particuology*, vol. 11, pp. 737–742, 2013.
 13. R.-H. Jie, G.-B. Guo, W.-G. Zhao, and S.-L. An, *Journal of Synthetic Crystals*, vol. 42, pp. 2144–2149, 2013.
 14. H. U. Lee, G. Lee, J. C. Park et al., *Chemical Engineering Journal*, vol. 240, pp. 91–98, 2014.
 15. Matthews R., 1993. Elsevier Science Publishers. pp. 121–139.
 16. Nurhidayatullaili Muhd Julkapli, Samira Bagheri, and Sharifah Bee Abd Hamid, *The Scientific World Journal*, Volume 2014, Article ID 692307.
 17. T.-D. Nguyen-Phan, V.H. Pham, T.V. Cuong, S.H. Hahn, E.J. Kim, J.S. Chung, S.H. Hur, E.W. Shin, *Mater. Lett.* 64 (2010) 1387–1390.
 18. Priyanka and V. C. Srivastava, *Industrial & Engineering Chemistry Research*, vol. 52, no. 50, pp. 17790–17799, 2013.
 19. Rahman MM, Khan BS, Marwani HM, Asiri AM, Alamry KA, Rub MA, Khan A, Khan AAP, Azum N, *J. Ind. Eng. Chem.* 20: 2278–2286, 2014.
 20. Saleh TA, Gupta VK, *J. Colloid Interface Sci.* 371: 101-106, 2012.
 21. R. Santos Fernández, G. Torres-Delgado, R. Castanedo-Pérez, J. Márquez-Marín, O. Zelaya-Ángel, , *International Materials Research Congress*, 2017.
 22. S. Sarkar and K. K. Chattopadhyay, *Physica E*, vol. 58, pp. 52–58, 2014.
 23. B. Shahmoradi, A. Maleki, and K. Byrappa, *Desalination & Water Treatment*, 2013.
 24. Shiragami T., S. Fukami & Y. Wada, *The Journal of Physical Chemistry* 97(Dec 9): 12882–12887, 1993.

25. Smith B.A., D.M. Waters, A.E. Faulhaber, M.A. Kreger, T.W. Roberti & J.Z. Zhang, Journal of Sol–Gel Science and Technology 9: 125–137, 1997.
26. T. Soltani and M. H. Entezari, Journal of Molecular Catalysis A, vol. 377, pp. 197–203, 2013.
27. L. Sun, Y. Shi, B. Li, X. Li, and Y. Wang, Polymer Composites, vol. 34, no. 7, pp. 1076–1080, 2013.
28. K. Ullah, Z.-D. Meng, S. Ye, L. Zhu, and W.-C. Oh, Journal of Industrial and Engineering Chemistry, vol. 20, no. 3, pp. 1035–1042, 2014.
29. J. Zhang, W. Liu, X. Wang, X. Wang, B. Hu, and H. Liu, Applied Surface Science, vol. 282, pp. 84–91, 2013.
30. Ziabari AA, Ghodsi FE, J. Alloy Compd. 509: 8748-8755, 2011.